

# Hydrological thresholds and basin control over paleoflood records in lakes

Daniel N. Schillereff\*, Richard C. Chiverrell, Neil Macdonald, and Janet M. Hooke

School of Environmental Sciences, Roxby Building, University of Liverpool, L69 7ZT Liverpool, UK

## ABSTRACT

The scarcity of long-term hydrological data is a barrier to reliably determining the likelihood of floods becoming more frequent and/or intense in a warmer world. Lake sediments preserve characteristic event layers, offering the potential to develop widely distributed and unique chronologies of historical floods. Inferring flood magnitude remains a greater challenge, previously overcome in part by analyzing sharply laminated polar or alpine sequences. Here we demonstrate an approach to obtain flood frequency and magnitude data from an unexploited resource, the largely visually homogeneous, organic sediments that typify most temperate lakes. The geochemical composition and end-member modeling of sediment trap and adjacent short core particle size data for Brotherswater (northwest England) discriminates the signature of infrequent, coarse-grained flood deposits from seasonal and longer term allogenic (enhanced discharge and sediment supply during winter) and autogenic (summer productivity, thermal mixing) depositional processes. Comparing the paleoflood reconstruction to local river discharges shows that hydrological thresholds censor event signature preservation, with 4 yr recurrence intervals detectable in delta-proximal sediments declining to 9 yr in the lake center. Event threshold (discharge) and process characterization are essential precursors to discerning flood magnitude from sediment archives. Implementation of our approach in globally prevalent temperate lakes offers a vast, unique repository of long-term hydrological data for hydrologists, climate modelers, engineers, and policy makers addressing future flood risks.

## INTRODUCTION

Attempts to address concerns that a warming climate may trigger more frequent and/or intense floods are hampered by a paucity of long-term observational data against which trends in hydrological extremes can be evaluated (IPCC, 2013). Lakes and their sediments are increasingly being used to generate annually and seasonally resolved paleohydrological data to assess flood frequency in relation to climatic drivers (Swierczynski et al., 2012; Wirth et al., 2013), but inferring flood magnitude from sediments remains a challenge (Schiefer et al., 2011; Kämpf et al., 2014). Reliably determining the minimum discharge for a discernible sedimentary imprint to be preserved is a key precursor to building a time series of river discharge from a lake sediment core; hydrological thresholds of this nature have only been established at annually laminated sites (Corella et al., 2014; Kämpf et al., 2014) and for sediment sequences comprising well-defined lithological contacts (Kämpf et al., 2012). Such well-stratified sediments are not ubiquitous: homogeneous, organic-rich materials dominate the Holocene stratigraphy of many non-alpine and non-polar lakes. In these lakes, visual discrimination of flood layers is challenging and interpreting flood indicators from micro X-ray fluorescence ( $\mu$ XRF)

data alone can be misleading (Schillereff et al., 2014). We demonstrate a systematic approach to determine hydrological thresholds at temperate lakes, which is a significant step toward accessing magnitude from this untapped archive. Data from a 16 month campaign of sediment trapping at Brotherswater (northwest England) are integrated with the recent depositional record and calibrated against gauged river flows (Common Era [CE] 1962–2014) to ascertain the basin controls over subdecadal- to event-scale sediment supply as autogenic (productivity, mixing regime) and allogenic (hydrological and sediment supply) processes affect the character and preservation of paleoflood laminations (Schillereff et al., 2014). Characterizing modes of deposition under flood and non-flood conditions by end-member (EM) analysis of the particle size distributions (PSDs) shows that variations in grain size are the most appropriate paleoflood metric.

## STUDY SITE AND METHODS

Brotherswater is a small (0.18 km<sup>2</sup>), mesotrophic, upland (altitude 158 m) lake with a large catchment-to-lake area (C:L 72:1) (Figs. 1A and 1B). Sediments enter through a single inflow and descend to a flat profundal zone (16 m depth) that dominates the lake and develops weak summer thermal stratification. Limited shallow waters reduce remobilization potential. Two moorings were established (August 2012–December 2013): 75 m from the inflow delta (site A, 12 m depth), and more

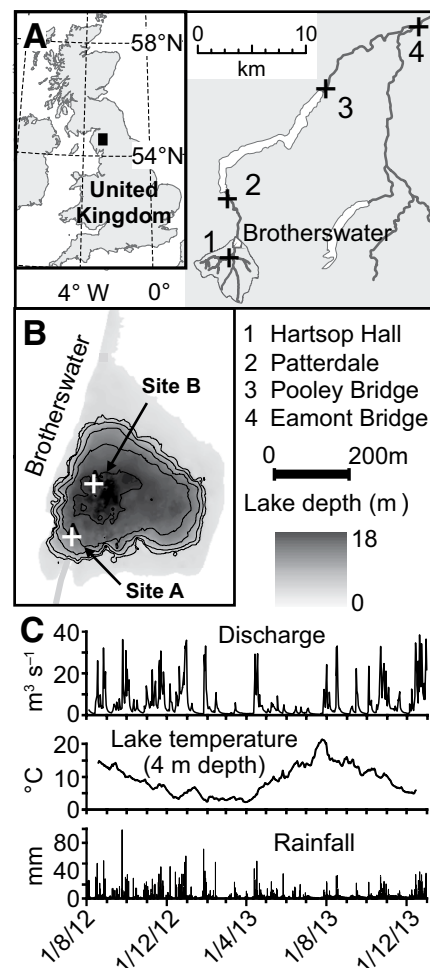


**Figure 1. A:** Location map of Brotherswater (northern England) and measurement stations. **B:** Bathymetry of Brotherswater (3 m contours) and sediment trap locations. **C:** Time series of daily maximum discharge (Patterdale), total daily rainfall (Hartsop Hall), and Brotherswater water temperature at site A.

distal (225 m; site B, 16 m depth) (Fig. 1B). Pairs of cylindrical traps (see the GSA Data Repository<sup>1</sup>) were suspended at three depths: near the lake bed collecting hyperpycnal flow deposition; the seasonal metalimnion (6–8 m)

<sup>1</sup>GSA Data Repository item 2016010, trap design, hydrometeorological and chronological data processing, Figure DR1 (age-depth data), Figure DR2 (proxy correlation matrix), Figure DR3 (monthly particle size distributions), Figure DR4 (comparison between gauging station records), and Table DR1 (monthly trapped sediment volumes), is available online at [www.geosociety.org/pubs/ft2016.htm](http://www.geosociety.org/pubs/ft2016.htm), or on request from [editing@geosociety.org](mailto:editing@geosociety.org) or Documents Secretary, GSA, P.O. Box 9140, Boulder, CO 80301, USA.

\*Current address: Department of Geography, King's Building, King's College London, WC2R 2LS London, UK; E-mail: [daniel.schillereff@kcl.ac.uk](mailto:daniel.schillereff@kcl.ac.uk).

for mesopycnal flows; and 4 m, also logging (HOBO U20-001-04 water level logger) water level and temperature at 10 min increments, for hypopycnal plumes. Recently accumulated (post-1960) lake sediments adjacent to the trap stations were retrieved using a gravity corer (BW11-2 and BW12-9), subsampled at narrow resolution of equivalent thickness (0.5 cm), and freeze dried. The homogeneous sediment matrix precluded the identification and subsampling of event laminations. Local daily precipitation data were obtained from Hartsop Hall (1997–2013) and maximum daily discharges ( $Q_{\max}$ ) were obtained for the Brotherswater outflow at Patterdale (1997–2013), Pooley Bridge (1976–2013), and Eamont Bridge (1962–2013) (Figs. 1A and 1C) (for methods, see the Data Repository). For the trap and core samples, we measured PSDs (Coulter LS 13 320 laser diffractor), geochemical composition (Bruker S2 Ranger energy dispersive-XRF), and organic carbon by thermogravimetric mass loss (150–530 °C) under a nitrogen atmosphere (PerkinElmer STA6000). Radiometric dating of both cores generated  $^{210}\text{Pb}$  chronologies corroborated by well-defined 1963 and 1986  $^{137}\text{Cs}$  and  $^{241}\text{Am}$  markers, which yielded chronological uncertainty of  $\pm 1\text{--}2$  yr (1970–2014) and  $\pm 4$  yr pre-1970 (see the Data Repository). PSDs were partitioned into statistical EMs using the R package EMMAgeo (Dietze and Dietze, 2013), with frequency statistics calculated using Folk and Ward (1957) geometric formulae.

## RESULTS AND INTERPRETATION

Rainfall and discharge during the monitoring period (August 2012–December 2013) reflected the longer term seasonal pattern, with higher average and peak flows in autumn and winter and a summer lull (Fig. 1C). Six rainfall-driven flows  $>30\text{ m}^3\text{ s}^{-1}$  were recorded; the peak was  $36.2\text{ m}^3\text{ s}^{-1}$ . For context, the exceptional 19–20 November 2009 event ( $R = 460$  yr; Miller et al., 2013) generated  $Q_{\max} = 61.4\text{ m}^3\text{ s}^{-1}$ . Sedimentation was higher near the inflow (Table DR1 in the Data Repository) and the mass accumulation rate shows strong similarity to river flow with more rapid accumulation in the upper and middle traps during autumn and winter than in spring and summer (Fig. 2), although rapid summer accumulation occurred at depth in the lake center ( $2.35\text{ mg cm}^{-2}\text{ d}^{-1}$ ) and 10 July–10 August 2013 at site A. Trapped materials become finer from delta proximal (P90: 150–250  $\mu\text{m}$ ) to distal settings (75–200  $\mu\text{m}$ ). At site A, the coarsest sediment was captured at upper and middle depths during autumn and winter, whereas particles were finer near the surface during summer (Fig. 2); fine-grained materials characterize summer sedimentation at site B. Ti and Zr maxima during autumn and winter 2012 indicate that catchment erosion is an important sediment source that declines during summer (Fig. 2). Ti and Zr

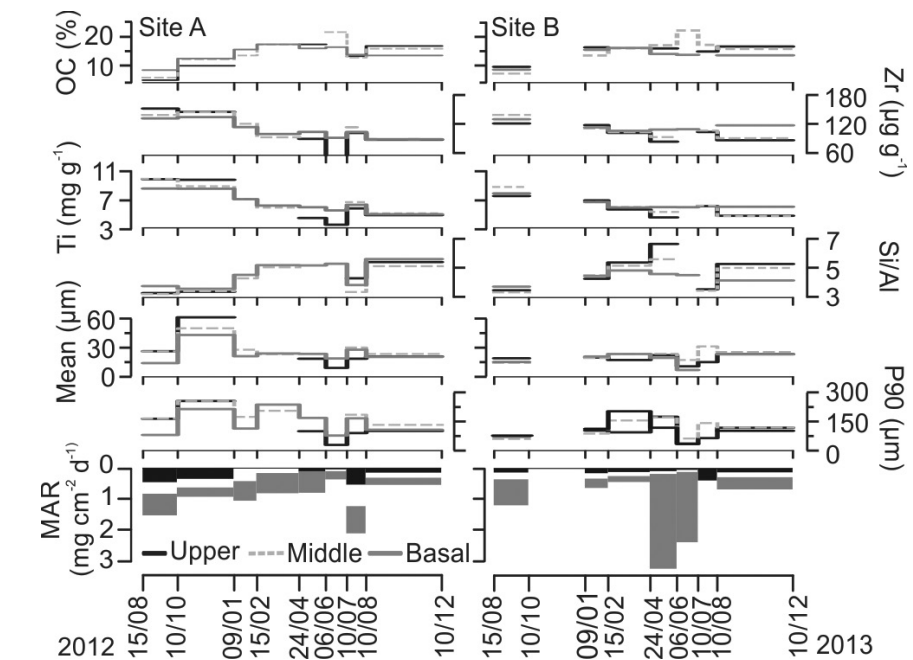


**Figure 2.** Intra-annual patterns in trapped sediments of organic carbon (OC), Zr, Ti, Si/Al ratio, mean and 90<sup>th</sup> percentile grain size, and mass accumulation rate (MAR).

correlate with other lithogenic elements (Al, K, Rb;  $R > 0.87$ ) and with fine to medium sand, but correlate negatively with silt (Fig. DR2). This absence of particle size fractionation (Taboada et al., 2006) negates their use as particle size indicators at Brotherswater. Reduced lithogenic elements and increased organic and Si contents during summer 2013 point to in-lake productivity influencing peak sedimentation. The Si/Al maximum April–June 2013 (Fig. 2) is indicative of a spring diatom bloom (Peinerud, 2000).

Trap samples reveal considerable particle size variability, with unimodal, bimodal, and polymodal PSDs (Fig. DR3) most likely reflecting different depositional mechanisms. EM modeling, which employs principal component and factor analyses to identify statistically similar particle size distributions, has helped decipher process links between sediment caliber and river flow (Fig. 3). EM decomposes the PSD into three groupings: EM1 (mode = 11  $\mu\text{m}$ ,  $\pm 1\sigma = 5\text{--}15\text{ }\mu\text{m}$ , 34% variance explained), EM2 (36  $\mu\text{m}$ , 15–83  $\mu\text{m}$ , 32%) and EM3 (194  $\mu\text{m}$ , 83–409  $\mu\text{m}$ , 33%) (Fig. 3A). Sedimentation during summer months is characterized by high EM1, the fine-grained, organic-rich fraction. EM2 persists throughout, presumably reflecting background accumulation. Trapped sediments display primary modes in the medium silt domain, but site A PSDs exhibited secondary modes in the coarse silt and fine to medium sand fractions (EM3). Higher flows at site A produced sand-rich distributions that contrast with better sorted, fine to medium silts deposited in other months. Persistent elevated but unexceptional flows 19–30

December 2012 (Fig. 1B) produced a coarse (P90 = 256  $\mu\text{m}$ ), negatively skewed distribution dominated by EM3 (January 2013; Fig. 3B). Higher but shorter duration peak flows on 24 July 2012 did not generate this PSD signature. The moderately coarse materials captured 10 August 2013 have a secondary sand mode and probably reflect elevated flow 28 July–07 August 2013. Their abrupt nature after 2 months of low rainfall appears to have mobilized large-caliber particles despite modest  $Q_{\max}$  ( $24.2\text{ m}^3\text{ s}^{-1}$ ). Conversely, higher flows 27–29 January 2013 ( $Q_{\max} = 33.1\text{ m}^3\text{ s}^{-1}$ ) delivered medium silts with less EM3 than January 2013 or August 2013, suggesting that event sequencing flushed coarser materials from temporary fluvial stores during December 2012.

Normalizing the trap PSD for mass accumulation and time produces annual-equivalent distributions that resemble EM2: a medium-silt primary mode and subdued coarse tail (Fig. DR3). The event-scale EM3 component (e.g., January 2013) blurs into background, indicating that coarse particles delivered during monitored high flows are masked by the regular deposition of clay and fine to medium silt. These data indicate that the threshold (T) for preserving a flood sedimentary signature in Brotherswater exceeds  $36.2\text{ m}^3\text{ s}^{-1}$ , the maximum discharge recorded during monitoring.

Extending this analysis to the cores (Fig. 3C) reveals the same EMs and likely process continuity between monitored and post-1960 sedimentation. Mean sediment accumulation since 1960 was  $0.57\text{ cm yr}^{-1}$  ( $1\sigma = 0.11$ ), meaning that the 0.5 cm equal-interval subsampling

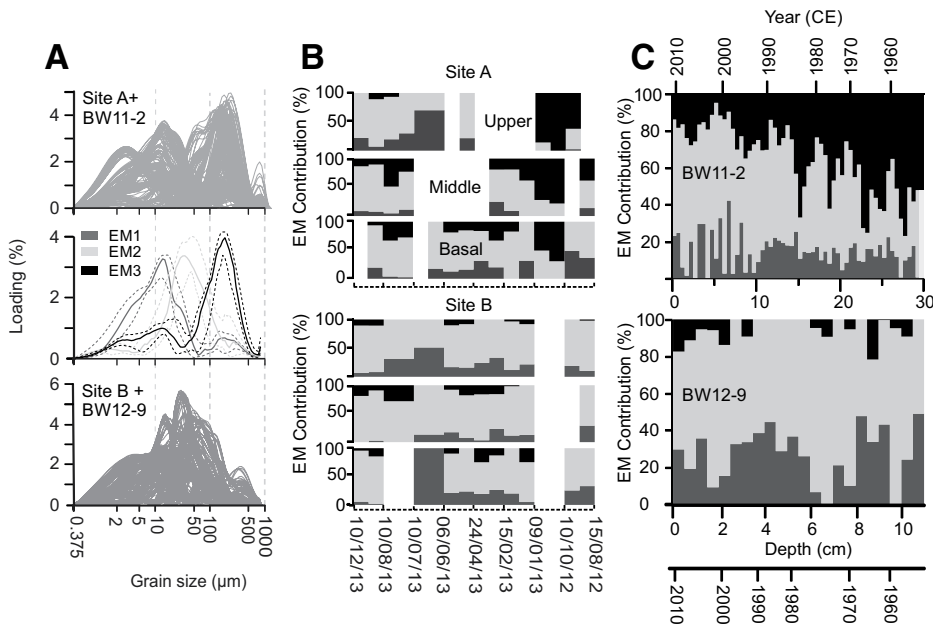


**Figure 3. A:** Particle size distributions for sediment trap and core samples and the partitioned end members (EM). **B:** The EM1–EM 3 loadings plotted against time for traps. **C:** The EM1–EM3 loadings plotted against time for cores.

necessitated by the visually homogeneous sediment column and inconspicuous depositional contacts approximates yearly accumulation. Thus, EM3 peaks in BW11–2 and BW12–9 are interpreted as flood laminations approaching annual resolution deposited under magnitudes  $>T$ , and likely substantially higher given the typically much greater EM3 proportion in the cores (Fig. 3C).

From 1960 to present, the sediment cores show variations in lithogenic elements (Ti, Zr), organic carbon, and algal (Si/Al) productivity and decreasing EM3 contribution (Figs. 3C and 4), reflecting a reduced supply of coarse material. This long-term trend is overprinted by episodic coarse events and has been filtered by expressing the P90 as residuals (P90<sub>res</sub>) from a Savitzky-Golay 11-point moving average (Fig. 4). Age probability distributions were calculated for the coarse deposits (peak P90<sub>res</sub>) using Bayesian software (Blaauw and Andrés Christen, 2011). For BW11–2, there is a temporal match between the 13 P90<sub>res</sub> peaks and floods in the gauged series where discharge exceeds  $39 \text{ m}^3 \text{ s}^{-1}$ ,  $66 \text{ m}^3 \text{ s}^{-1}$ , and  $70 \text{ m}^3 \text{ s}^{-1}$  at Patterdale, Pooley, and Eamont (Fig. 4), respectively. Overall, discharges increase down-catchment, but the comparative scaling of peak flows is consistent between stations during the overlap periods (Fig. DR4). Only 8 P90<sub>res</sub> peaks appear in BW12–9; within the chronological uncertainty these include the 1964, 1968, and 1974–1975 floods, and only 2 events detected since 2000. Thus, there is underrepresentation of floods in the sediment record below these hydrological thresholds, a factor exacerbated

away from the inflow as sediment dispersal and accumulation rates decline.

### BASIN REGULATION OF SEDIMENT DYNAMICS

The geochemical composition of trap samples highlight a substantial terrigenous contribution; high C:L ratio, abundant available sediment, and flashy discharge contribute to this flux. Monitoring for 16 months is short in duration compared to millennial-scale sediment records, but enables the basin control to be

characterized: winter increases in clastic materials and late-spring algal and summer organic productivity regulate the sediment volume and composition (Fig. 2).

Optimal coring locations depend on research objectives, and within-lake sediment routing is critical for paleoflood studies (Wilhelm et al., 2015). At Brotherswater, high flows introduce water warmer than that of the lake (Fig. 1C); the diffusion of these less dense hypopycnal plumes represents the dominant sediment dispersal pathway, differing from cold, dense winter hyperpycnal flows dispersing materials in turbulent suspension across the profundal basin in polar and montane lakes (Gilbert et al., 2006; Cockburn and Lamoureux, 2008; Roop et al., 2015). The December 2012 event delivered more coarse material to the upper traps (Fig. 3B), censoring the flood record with increasing distance from the inflow. The lack of hyperpycnal behavior at Brotherswater reduces chances of sediment-laden underflows bypassing the inflow sector. Summer peak flows (August 2013) delivered coarser particles to the middle and low water column (Figs. 2 and 3B), indicative of interflows dispersing at the summer thermocline (Desloges and Gilbert, 1994; Kämpf et al., 2014). Our monitoring shows that deposition in Brotherswater is controlled by distance from inflow, and neither sediment focusing nor local sediment remobilization in deltaic zones influence flood deposit preservation (Kämpf et al., 2014), highlighting that a delta-proximal coring site should yield the optimal paleoflood record.

### PALEOFLOOD HISTORIES FROM LAKE SEDIMENTS

Evaluating autogenic and allogenic depositional processes offers critical insight into rela-

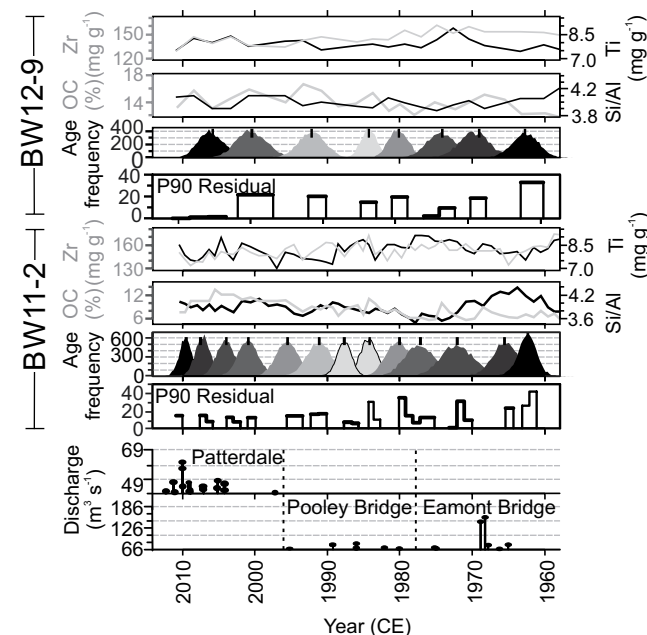


**Figure 4.** Proxy data of sediment regime plotted alongside P90 residuals for the period CE 1960–2012 identifying flood deposits at BW11–2 and BW12–9. Their Bayesian age probability functions and weighted mean ages (black bar) are compared with daily discharges  $>T$  (threshold) for three local gauging stations. OC—organic carbon.

tionships between proxy record and river discharge. At Brotherswater, the volcanic bedrock exerts a local control, yielding a lake sediment geochemical composition insensitive to particle size fractionation, which precludes the detection of flood laminations using  $\mu$ XRF core scanning. Geochemical particle size proxies require validation on a site-by-site basis. Coarse layers reflecting non-flood processes in lakes (e.g., slope instability, internal slumping) can be identified from sharp, potentially erosive, contacts and particle size grading within units (Swierczynski et al., 2012; Corella et al., 2014; Kämpf et al., 2014). For settings lacking a clear visual stratigraphy, employing sediment traps to discern flow pathways and verify the flood provenance of a deposit is essential (Figs. 2 and 3).

Chronological precision of the Brotherswater paleoflood record is inevitably constrained by the analytical resolution and uncertainty in the age-depth model; multiple floods that occurred during the broadly annual timespan of individual subsamples cannot be separated in the sediment record, such as several floods in the period 1966–1968. Subdecadal variability in lithogenic supply and biotic activity (Fig. 4) can potentially adjust thresholds and modify associations between river flow and flood signature. The December 2012 deposit was significantly coarser than other shorter, higher discharge events: the area under the hydrograph appears to govern the caliber of flood-derived sediment, and the muted signal from short-lived events affirms that complex discharge-PSD relationships noted for Canadian Arctic lakes (Cockburn and Lamoureux, 2008) are present in non-nival settings. Quantifying this relationship must also account for event sequencing, emptying or charging sediment stores so subsequent floods have limited or greater sedimentological significance, respectively (Schiefer et al., 2011), seen by the absence of coarse particles in February 2013 despite high flows in late January.

Integrating the trapping and core data sheds light on hydrogeomorphic processing at interannual scales. Peak flows during the monitoring period appear insufficient to leave a discernible particle size signature, illustrating that background sedimentation is censoring the record at flows  $<36.2 \text{ m}^3 \text{ s}^{-1}$ . The longer paleoflood record shows a good temporal match with station-specific discharges  $>T$  (Fig. 4). The preservation of 13 signatures in BW11–2 suggests that events with a 4 yr recurrence interval yield an imprint detectable in the basal sediments. Fewer coarse peaks at more distal settings show that the event frequency required to affect the lake center is longer,  $\sim 9$  yr. Our method allows both optimal coring locations and minimum event thresholds to be established.

An approach to obtain quantitative paleoflood data from globally prevalent temperate lakes characterized by homogeneous sediments is demonstrated, accessing a hitherto unexploited archive. Integrating systematic process monitoring and calibration of the depositional record to river discharge is essential to obtain site-specific understanding of factors controlling event signature preservation and is an approach applicable across lacustrine, fluvial, and near-shore marine depocenters. Its implementation across the widely distributed range of equivalent lakes offers an unprecedented data set for more reliably evaluating trends in hydrological extremes, testing model projections of future flood risk, establishing structural design criteria, and informing flood risk mitigation strategies.

#### ACKNOWLEDGMENTS

Funding was provided by a University of Liverpool Graduate Bursary, and Peter Appleby (Liverpool) provided radioisotope dating. National River Flow Archive (UK) and British Atmospheric Data Centre data sources are acknowledged. Jeff Warburton, John Boyle, and five anonymous reviewers provided constructive comments on earlier versions.

#### REFERENCES CITED

- Blaauw, M., and Andrés Christen, J., 2011, Flexible paleoclimate age-depth models using an autoregressive gamma process: Bayesian Analysis, v. 6, p. 457–474, doi:10.1214/ba/1339616472.
- Cockburn, J.M.H., and Lamoureux, S.F., 2008, Inflow and lake controls on short-term mass accumulation and sedimentary particle size in a High Arctic lake: Implications for interpreting varved lacustrine sedimentary records: *Journal of Paleolimnology*, v. 40, p. 923–942, doi:10.1007/s10933-008-9207-5.
- Corella, J.P., Benito, G., Rodríguez-Lloveras, X., Brauer, A., and Valero-Garcés, B.L., 2014, Annually-resolved lake record of extreme hydro-meteorological events since AD 1347 in NE Iberian Peninsula: *Quaternary Science Reviews*, v. 93, p. 77–90, doi:10.1016/j.quascirev.2014.03.020.
- Desloges, J.R., and Gilbert, R., 1994, Sediment source and hydroclimatic inferences from glacial lake sediments: The postglacial sedimentary record of Lillooet Lake, British Columbia: *Journal of Hydrology*, v. 159, p. 375–393, doi:10.1016/0022-1694(94)90268-2.
- Dietze, M., and Dietze, E., 2013, EMMAgeo: End-member modelling algorithm and supporting functions for grain-size analysis, R package version 0.9.1: <http://cran.r-project.org/web/packages/EMMAgeo/EMMAgeo.pdf>.
- Folk, R.L., and Ward, W.C., 1957, Brazos River bar (Texas); a study in the significance of grain size parameters: *Journal of Sedimentary Research*, v. 27, p. 3–26, doi:10.1306/74D70646-2B21-11D7-8648000102C1865D.
- Gilbert, R., Crookshanks, S., Hodder, K.R., Spagnol, J., and Stull, R.B., 2006, The record of an extreme flood in the sediments of montane Lillooet Lake, British Columbia: Implications for paleoenvironmental assessment: *Journal of Paleolimnology*, v. 35, p. 737–745, doi:10.1007/s10933-005-5152-8.

- IPCC (Intergovernmental Panel on Climate Change Working Group), 2013, *Climate change 2013: The physical science basis*: Cambridge, UK, Cambridge University Press, 1535 p.
- Kämpf, L., Brauer, A., Dulski, P., Lami, A., Marchetto, A., Gerli, S., Ambrosetti, W., and Guizzoni, P., 2012, Detrital layers marking flood events in recent sediments of Lago Maggiore (N. Italy) and their comparison with instrumental data: *Freshwater Biology*, v. 57, p. 2076–2090, doi:10.1111/j.1365-2427.2012.02796.x.
- Kämpf, L., Brauer, A., Swierczynski, T., Czymzik, M., Mueller, P., and Dulski, P., 2014, Processes of flood-triggered detrital layer deposition in the varved Lake Mondsee sediment record revealed by a dual calibration approach: *Journal of Quaternary Science*, v. 29, p. 475–486, doi:10.1002/jqs.2721.
- Miller, J.D., Kjeldsen, T.R., Hannaford, J., and Morris, D.G., 2013, A hydrological assessment of the November 2009 floods in Cumbria, UK: *Hydrology Research*, v. 44, p. 180–197, doi:10.2166/nh.2012.076.
- Peinerud, E.K., 2000, Interpretation of Si concentrations in lake sediments: Three case studies: *Environmental Geology*, v. 40, p. 64–72, doi:10.1007/PL00013330.
- Roop, H.A., Dunbar, G.B., Levy, R., Vandergoes, M.J., Forrest, A.L., Walker, S.L., Purdie, J., Upton, P., and Whinney, J., 2015, Seasonal controls on sediment transport and deposition in Lake Ohau, South Island, New Zealand: Implications for a high-resolution Holocene palaeoclimate reconstruction: *Sedimentology*, v. 62, p. 826–844, doi:10.1111/sed.12162.
- Schiefer, E., Gilbert, R., and Hassan, M.A., 2011, A lake sediment-based proxy of floods in the Rocky Mountain Front Ranges, Canada: *Journal of Paleolimnology*, v. 45, p. 137–149, doi:10.1007/s10933-010-9485-6.
- Schillereff, D.N., Chiverrell, R.C., Macdonald, N., and Hooke, J.M., 2014, Flood stratigraphies in lake sediments: A review: *Earth-Science Reviews*, v. 135, p. 17–37, doi:10.1016/j.earscirev.2014.03.011.
- Swierczynski, T., Brauer, A., Lauterbach, S., Martin-Puertas, C., Dulski, P., von Grafenstein, U., and Rohr, C., 2012, A 1600 yr seasonally resolved record of decadal-scale flood variability from the Austrian pre-Alps: *Geology*, v. 40, p. 1047–1050, doi:10.1130/G33493.1.
- Taboada, T., Cortizas, A.M., García, C., and García-Rodeja, E., 2006, Particle-size fractionation of titanium and zirconium during weathering and pedogenesis of granitic rocks in NW Spain: *Geoderma*, v. 131, p. 218–236, doi:10.1016/j.geoderma.2005.03.025.
- Wilhelm, B., Sabatier, P., and Arnaud, F., 2015, Is a regional flood signal reproducible from lake sediments? *Sedimentology*, v. 62, p. 1103–1117, doi:10.1111/sed.12180.
- Wirth, S.B., Gilli, A., Simonneau, A., Ariztegui, D., Vannièrè, B., Glur, L., Chapron, E., Magny, M., and Anselmetti, F.S., 2013, A 2000 year long seasonal record of floods in the southern European Alps: *Geophysical Research Letters*, v. 40, p. 4025–4029, doi:10.1002/grl.50741.

Manuscript received 13 August 2015

Revised manuscript received 29 October 2015

Manuscript accepted 31 October 2015

Printed in USA